

Construction of a Blue Copper Analogue through Iterative Rational Protein Design Cycles Demonstrates Principles of Molecular Recognition in Metal Center Formation

Homme W. Hellinga

Contribution from the Department of Biochemistry, Duke University Medical Center, Durham, North Carolina 27710

Received January 5, 1998

Abstract: The construction and characterization of a series of proteins in which the Blue Copper CysHis₂Met primary coordination sphere was placed in various orientations within the hydrophobic core of thioredoxin has allowed exploration of the principles of molecular recognition between proteins and metals. An automated rational protein design algorithm predicted structurally suitable locations for these centers without use of either a potential preexisting binding site or any structural or sequence homology between the thioredoxin host and known Blue Copper proteins. A series of four primary designs and 32 variants were constructed. It was necessary to surround the designed primary coordination sphere with a hydrophobic shell to ensure the absence of potential alternative coordinating residues. Formation of a stable Cu(II)-thiolate bond required destabilization of a normally favored redox reaction in which the thiol is oxidized to a disulfide. This was achieved by more deeply burying the coordinating cysteine, presumably via a mechanism in which the free energy of protein unfolding opposes the competing redox reaction. The distorted tetrahedral coordination geometry of the Cu(II) complex is unstable with respect to a competing tetragonal geometry resulting from incorporation of bound water. Although natural systems appear to sterically exclude such water binding, this exclusion mechanism was not successfully reproduced in the designs presented here. Instead, a suitably placed small cavity allowed a strong, exogenous ligand, such as azide, to be introduced axially, which competitively stabilizes the tetrahedral geometry corresponding to a "Type 1.5" Blue Copper complex in favor of the tetragonally bound water. This iterative rational design study demonstrates that destabilization of competing reactions ("negative design") is a crucial, if cryptic, aspect of molecular recognition in proteins, and that proteins have evolved a variety of mechanisms that impose negative design constraints.

Introduction

Rational design is rapidly emerging as a tool to investigate the general principles in the relationship between protein structure and function.¹ One approach starts with the simplest molecular model and iteratively introduces further levels of complexity as guided by the experimental results.^{1c} This strategy aims to uncover a minimally sufficient set of components that dominate the formation of the desired structure or function. The de novo design of metal centers in proteins is well suited to this approach,² because the factors that control their structure and reactivity can be classified into a clear hierarchy.³ The properties of the metal center are dominated by the choice, number, and geometry of ligands in the primary coordination sphere. The next most dominant factors are the

interactions between the primary coordination sphere and its immediate surroundings (secondary coordination shell). The final level of modulation arises from long-range interactions dispersed throughout the protein. An iterative strategy can therefore be devised that starts with the construction of just the primary coordination sphere and progressively introduces long-range interactions.

The de novo introduction of metal centers in proteins of known structure provides a starting point for such iterative design cycles. Designs can be generated by an automated design algorithm, Dezymer,⁴ which takes into account only the geometry of the primary coordination sphere and its approximate steric compatibility with the surrounding protein matrix. Using this procedure, several different metal centers have been introduced at various locations in the hydrophobic core of *E. coli* thioredoxin,⁵ a protein normally devoid of metal sites,⁶ including an Fe₄S₄ cluster,⁷ a mononuclear iron-sulfur center,⁸

(1) (a) Bryson, J. W.; Betz, S. F.; Lu, H. S.; Suich, D. J.; Zhou, H. X.; O'Neil, K. T.; DeGrado, W. F. *Science* **1995**, *270*, 935–941. (b) Dahiyat, B. I.; Mayo, S. L. *Science* **1997**, *278*, 82–87. (c) DeGrado, W. F.; Wasserman, Z. R.; Lear, J. D. *Science* **1989**, *243*, 622–628.

(2) Tainer, J. A.; Roberts, V. A.; Getzoff, E. D. *Curr. Opin. Biotech.* **1991**, *2*, 582–591. (b) Tainer, J. A.; Roberts, V. A.; Getzoff, E. D. *Curr. Opin. Biotech.* **1992**, *3*, 378–387. (c) Regan, L. *Annu. Rev. Biophys. Biomol. Struct.* **1993**, *22*, 257–281. (d) Regan, L. *Trends Biochem. Sci.* **1995**, *20*, 280–285. (e) Hellinga, H. W. In *Protein Engineering: Principles and Practice*; J. L. Cleland and C. S. Craik, Eds.; Wiley-Liss: New York, 1996; p 369–398. (f) Hellinga, H. W. *Curr. Opin. Biotech.* **1996**, *7*, 437–441. (g) Lu, Y.; Valentine, J. S. *Curr. Opin. Struct. Biol.* **1997**, *7*, 495–500. (h) Hellinga, H. W. *Folding Design* **1998**, *3*, R1–R8.

(3) Holm, R. H.; Kennepohl, P.; Solomon, E. I. *Chem. Rev.* **1996**, *96*, 2239–2314.

(4) Hellinga, H. W.; Richards, F. M. *J. Mol. Biol.* **1991**, *222*, 763–785. (5) Katti, S. K.; LeMaster, D. M.; Eklund, H. *J. Mol. Biol.* **1990**, *212*, 167–184.

(6) (a) Holmgren, A. *Structure* **1995**, *3*, 239–243. (b) Martin, J. L. *Structure* **1995**, *3*, 245–250.

(7) Coldren, C. D.; Hellinga, H. W.; Caradonna, J. P. *Proc. Natl. Acad. Sci. U.S.A.* **1997**, *94*, 6635–6640.

(8) Benson, D. E.; Wisz, M. S.; Liu, W.; Hellinga, H. W. *Biochemistry* **1998**, *37*, 7070–7076.

a primitive iron-based superoxide dismutase,⁹ and a small family of Cys₂His₂ zinc sites.¹⁰ For these centers, the construction of a geometrically correct, sterically compatible primary coordination sphere is sufficient to reproduce the dominant features of their electronic structure and reactivity. This is not the case for Blue Copper centers, however, as was shown previously.¹¹ Here it is demonstrated through the construction of an iterative, progressive series of designs that for Blue Copper centers one must introduce additional, long-range interactions, the primary function of which is the suppression of competing coordination states and redox reactivities.

Blue Copper centers have been found in a variety of proteins,¹² including electron transport proteins and multi-copper enzymes,¹³ and are closely related to the binuclear copper centers found in cytochrome *c* oxidase.¹⁴ High-resolution X-ray structural studies,¹⁵ spectroscopic studies,¹⁶ protein engineering,¹⁷ and synthetic models¹⁸ have led to an increasingly detailed picture of the coordination geometry and electronic structure of these sites. Cu(II) is coordinated by a cysteine S_γ thiolate, two histidines N_δ atoms, and typically a methionine S_δ thioether, arranged in a distorted tetrahedron. The Cu(II) is located in the trigonal plane formed by three strong equatorial CysHis₂ ligands, with the methionine forming a weak axial bond. Compared with most small Cu(II) coordination compounds, the Blue Copper centers have a very unusual electronic structure. Their electronic absorption spectra are dominated by an absorbance at 600 nm that is at least an order of magnitude larger (2–6 mM⁻¹cm⁻¹) than usually found.¹⁶ Their electron paramagnetic resonance spectra show a very small value of the Cu(II) hyperfine splitting in the g_{||} region. Both these features are now understood to be the consequence of the covalent, delocalized character of the bonding interactions in this site, dominated by a strong bond between the copper and the thiolate, resulting in a sulfur to Cu(II) ligand-to-metal charge transfer (LMCT) that gives rise to the strong absorbance at 600 nm.¹⁶

Studies on synthetic models¹⁸ and engineered variants of copper-binding proteins^{19–25} have shown that the formation of a stable Blue Copper center can be opposed by several alternative reactivities and coordination geometries. First, a highly favored redox reaction in which the mercaptide is oxidized to a disulfide competes with the formation of the Cu(II)-thiolate bond.¹⁸



Second, three different types of four-coordinate geometries have been identified^{17,25} (Figure 1): Type 1 centers are the

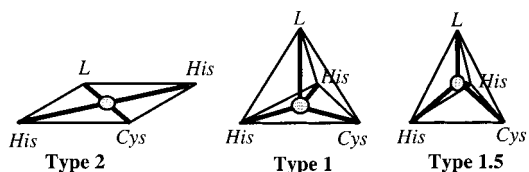


Figure 1. The three types of coordination geometries observed in four-coordinate Cu(II)-thiolate binding sites in proteins where three of the ligands are CysHis₂ and the fourth, *L*, can vary both in character and relative position (see text).

natural Blue Copper centers, in which the copper is located approximately within the trigonal plane formed by the three strong His₂Cys ligands with a weak axial methionine; type 2 centers are planar and tetragonal and correspond to the most stable way of arranging four ligands around Cu(II), in the absence of other factors;²⁶ type 1.5 centers have been found in engineered variants of Blue Copper centers^{31–42} in which a strong axial ligand replaces the weak methionine, thereby

(20) (a) den Blaauwen, T.; van der Kamp, M.; Canters, G. W. *J. Am. Chem. Soc.* **1991**, *113*, 5050–5052. (b) den Blaauwen, T.; Canters, G. W. *J. Am. Chem. Soc.* **1993**, *115*, 1121–1129. (c) den Blaauwen, T.; Hoitink, C. W.; Canters, G. W.; Han, J.; Loehr, T. M.; Sanders-Loehr, J. *Biochemistry* **1993**, *32*, 12455–12464. (d) Danielsen, E.; Bauer, R.; Hemmingsen, L.; Bjerrum, M. J.; Butz, T.; Tröger, W.; Canters, G. W.; Blaauwen, T. d.; van Pouderooyen, G. *Eur. J. Biochem.* **1995**, *233*, 554–560. (e) Hammann, C.; van Pouderooyen, G.; Nar, H.; Rüh, F.-X. G.; Messerschmidt, A.; Huber, R.; den Blaauwen, T.; Canters, G. W. *J. Mol. Biol.* **1997**, *266*, 357–366. (f) van Pouderooyen, G.; den Blaauwen, T.; Reedijk, J.; Canters, G. W. *Biochemistry* **1996**, *35*, 13205–13211.

(21) (a) Karlsson, B. G.; Nordling, M.; Pascher, T.; Tsai, L.-C.; Sjölin, L.; Lundberg, L. G. *Protein Eng.* **1991**, *4*, 343–349. (b) Chang, T. K.; Iverson, S. A.; Rodrigues, C. G.; Kiser, C. N.; Lew, A. Y. C.; Germanas, J. P.; Richards, J. H. *Proc. Natl. Acad. Sci. U.S.A.* **1991**, *88*, 1325–1329. (c) Di Bilio, A. J.; Chang, T. K.; Malmström, B. G.; Gray, H. B. *Inorg. Chim. Acta* **1992**, *198–200*, 145–148. (d) Murphy, L. M.; Strange, R. W.; Karlsson, B. G.; Lundberg, L. G.; Pascher, T.; Reinhammar, B.; Hasnain, S. S. *Biochemistry* **1993**, *32*, 1965–1975. (e) Coremans, J. W. A.; Poluektov, O. G.; Groenen, E. J. J.; Warmerdam, G. C. M.; Canters, G. W.; Nar, H.; Messerschmidt, A. *J. Phys. Chem.* **1996**, *100*, 19706–19713. (f) Kroes, S. J.; Hoitink, C. W.; Andrew, C. R.; Ai, J.; Sanders-Loehr, J.; Messerschmidt, A.; Hagen, W. R.; Canters, G. W. *Eur. J. Biochem.* **1996**, *240*, 342–351.

(22) (a) Vidakovic, M.; Germanas, J. P. *Angew. Chem., Int. Ed. Engl.* **1995**, *34*, 1622–1624. (b) Bonander, N.; Karlsson, B. G.; Vännegård, T. *Biochemistry* **1996**, *35*, 2429–2436.

(23) (a) van Pouderooyen, G.; Andrews, C. R.; Loehr, T. M.; Sanders-Loehr, J.; Mazumdar, S.; Hill, H. A. O.; Canters, G. W. *Biochemistry* **1996**, *35*, 1397–1407. (b) Germanas, J. P.; Di Bilio, A. J.; Gray, H. B.; Richards, J. H. *Biochemistry* **1993**, *32*, 7698–7702.

(24) (a) Romero, A.; Hoitink, C. W. G.; Nar, H.; Huber, R.; Messerschmidt, A.; Canters, G. W. *J. Mol. Biol.* **1993**, *229*, 1007–1021. (b) Tsai, L.-C.; Bonander, N.; Harata, K.; Karlsson, G.; Vännegård, T.; Langer, V.; Sjölin, L. *Acta Crystallogr.* **1996**, *D52*, 950–958. (c) Karlsson, G. G.; Tsai, L. C.; Nar, H.; Sanders-Loehr, J.; Bonander, N.; Langer, V.; Sjölin, L. *Biochemistry* **1997**, *36*, 4089–4095.

(25) (a) Lu, Y.; Gralla, E. B.; Roe, J. A.; Valentine, J. S. *J. Am. Chem. Soc.* **1992**, *114*, 3560–3562. (b) Lu, Y.; LaCroix, L. B.; Soloway, M. D.; Solomon, E. I.; Bender, C. J.; Peisach, J.; Roe, J. A.; Gralla, E. B.; Valentine, J. S. *J. Am. Chem. Soc.* **1993**, *115*, 5907–5918.

(26) (a) Hathaway, B. J.; Billing, D. E. *Coord. Chem. Rev.* **1970**, *5*, 143–207. (b) Gazo, J.; Bersuker, I. B.; Garaj, J.; Kabesová, M.; Kohout, J.; Langfelderová, H.; Melník, M.; Serátor, M.; Valach, F. *Coord. Chem. Rev.* **1976**, *19*, 253–297.

(27) Hellinga, H. W. *Proc. Natl. Acad. Sci. U.S.A.* **1997**, *94*, 10015–10017.

(28) (a) Hecht, M. H.; Richardson, J. S.; Richardson, D. C.; Ogden, R. C. *Science* **1990**, *249*, 884–891. (b) Richardson, J. S.; Richardson, D. C.; Tweedy, N. B.; Gernert, K. M.; Quinn, T. P.; Hecht, M. H.; Erickson, B. W.; Yan, Y.; McClain, R. D.; Donlan, M. E.; Surles, M. C. *Biophys. J.* **1992**, *63*, 1186–1209. (c) Quinn, T. P.; Tweedy, N. B.; Williams, R. W.; Richardson, J. S.; Richardson, D. C. *Proc. Natl. Acad. Sci. U.S.A.* **1994**, *91*, 8747–8751.

(29) Gill, S. C.; Hippel, P. H. v. *Anal. Biochem.* **1989**, *182*, 319–326.

(30) Ellman, G. L. *Arch. Biochem. Biophys.* **1959**, *82*, 70–77.

(31) Langsetmo, K.; Fuchs, J. A.; Woodward, C. *Biochemistry* **1991**, *30*, 7603–7609.

(32) Hellinga, H. W.; Wynn, R.; Richards, F. M. *Biochemistry* **1992**, *31*, 11203–11209.

(9) Pinto, A. L.; Hellinga, H. W.; Caradonna, J. P. *Proc. Natl. Acad. Sci. U.S.A.* **1997**, *94*, 5562–5567.

(10) Wisz, M. S.; Garrett, C. Z.; Hellinga, H. W. *Biochemistry* **1998**, *37*, 8269–8277.

(11) Hellinga, H. W.; Caradonna, J. P.; Richards, F. M. *J. Mol. Biol.* **1991**, *222*, 787–803.

(12) Sykes, A. G. *Adv. Inorg. Chem.* **1991**, *36*, 377–408.

(13) Solomon, E. I.; Sundaram, U. M.; Machonkin, T. E. *Chem. Rev.* **1996**, *96*, 2563–2605.

(14) Tsukihara, T.; Aoyama, H.; Yamashita, E.; Tomizaki, T.; Yamaguchi, H.; Shinzawa-Itoh, K.; Nakashima, R.; Yaono, R.; Yoshikawa, S. *Nature* **1995**, *269*, 1069–1074.

(15) (a) Adman, E. T. *Adv. Prot. Chem.* **1991**, *42*, 145–197. (b) Adman, E. T. *Curr. Opin. Struct. Biol.* **1991**, *1*, 895–904.

(16) (a) Solomon, E. I.; Baldwin, M. J.; Lowery, M. D. *Chem. Rev.* **1992**, *92*, 521–542. (b) Solomon, E. I.; Lowery, M. D.; LaCroix, L. B.; Root, D. E. *Methods Enzymol.* **1993**, *226*, 1–33.

(17) Canters, G. W.; Gilardi, G. *FEBS Lett.* **1993**, *325*, 39–48.

(18) Kitajima, N. *Adv. Inorg. Chem.* **1992**, *39*, 1–77.

(19) (a) Mizoguchi, T. J.; Bilio, A. J. D.; Gray, H. B.; Richards, J. H. *J. Am. Chem. Soc.* **1992**, *114*, 10076–10078. (b) Faham, S.; Mizoguchi, T. J.; Adman, E. T.; Gray, H. B.; Richards, J. H.; Rees, D. C. *J. Biol. Inorg. Chem.* **1997**, *2*, 464–469.

moving the copper out the trigonal plane of the type 1 centers²⁴ to form a coordination geometry that is more tetrahedral in character. The thiolate complexes of these three types can be readily distinguished by their electronic absorption spectra on the basis of the relative intensities and energies of the thiolate→Cu(II) LMCT bands.^{17,25} In type 1 sites the dominant LMCT is typically observed at ~600 nm; type 2 sites show a characteristic LMCT at 400 nm; type 1.5 sites are characterized by two contributions at 420–450 and 540–600 nm.

The design of Blue Copper centers requires the control of specificity. The desired state (the Blue Copper center) has to have the lowest free energy, and there has to be a large free energy difference between it and the next available state.²⁷ In an energy landscape consisting of several competing states, there are two ways to achieve this arrangement: *raising* the free energy of the competing states, or *lowering* that of the desired state. Here I present how an iterative design procedure can be used to experimentally define dominant competing states and to explore factors that manipulate the energy landscape of the Blue Copper metalloprotein complex by introducing or utilizing structural features that either raise the free energy of the experimentally characterized competing state(s) (“negative design”²⁸) or lower that of the desired state (“target state optimization”).

Materials and Methods

Construction and Purification of Mutant Proteins. Thioredoxin mutants (Trx[Bc]) were constructed by oligonucleotide-directed mutagenesis in M13 as described previously.¹¹ To overexpress the proteins, the mutant genes were recloned as C-terminal fusions with Maltose Binding Protein, separated by a flexible linker. The fully reduced, metal-free apo form of this protein is readily purified by affinity chromatography, as has been described in detail previously.⁸ The resulting protein was pure as judged by sodium dodecyl sulfate/polyacrylamide electrophoresis (SDS/PAGE) and staining an overloaded gel with Coomassie Blue. Protein concentrations were determined spectrophotometrically by measuring the 280-nm absorbance of the purified fusion protein ($\epsilon_{280} = 84 \text{ mM}^{-1}\text{cm}^{-1}$, as determined experimentally²⁹). Free thiol was determined by Ellman’s method.³⁰ Typical yields were 75–100 of mg pure fusion protein per liter of culture and 0.8–0.95 free thiols per protein.

All metal binding sites were constructed in a mutated background containing four additional mutations: an Asp2Ala mutation to remove an adventitious surface Cu(II) site known to exist at the amino terminus;^{5,11} a Cys32Ser, Cys35Ser double mutant to remove the native disulfide bridge, leaving the cysteine in the designed metal binding site as the only thiol-containing residue; and an Asp26Ala mutation that is known to significantly increase the stability of the folded form.³¹

Assessment of Structure. A genetic assay was used to test for the formation of folded protein.³² Wild-type thioredoxin is absolutely required for the growth of phage M13. M13 recombinants carrying thioredoxin variants³³ can be tested for growth on a nonpermissive *Escherichia coli* strain deleted for *trxA* (A307). Because the redox activity of thioredoxin is not required for this phenotype, a Cys32Ser-Cys25Ser double mutant (such as the Trx[Bc]-0.0 construct, see Table 1) supports M13 growth on A307. Detailed measurements of the changes in the free energies of protein folding will be presented elsewhere.

Formation and Analysis of Metal Complexes. Metal complexes were formed by successive additions of free metal dissolved in water to apoprotein solutions (MBP-TRX fusions), and the resulting electronic absorbance spectra were measured at room temperature with a Hitachi-2000 UV–Vis spectrophotometer. Where appropriate, this was done anaerobically in a Schlenk line, with use of a sealed cuvette (Hellma)

(33) In these recombinant phages, the mutant proteins are expressed as single thioredoxin domains (i.e., not as MBP fusions).

Table 1. List of All Constructs

construct ^a	mutations ^b
Trx[Bc]-0.0 ^c	Asp2Ala, Cys32Ser, Cys35Ser, Asp26Ala
Trx[Bc]-1.1 ^{d,e}	Trx[Bc]-0.0 + Leu7Cys, Val12His, Phe16His, Leu58Met
Trx[Bc]-2.1	Trx[Bc]-1.1 + Asp15Leu
Trx[Bc]-2.2	Trx[Bc]-1.1 + Asp9Leu
Trx[Bc]-2.3	Trx[Bc]-1.1 + Asp9Leu, Thr66Ile
Trx[Bc]-2.4	Trx[Bc]-1.1 + Asp9Leu, Asp15Leu, Thr66Ile
Trx[Bc]-3.1 ^e	Trx[Bc]-0.0 + Leu58Cys, Phe12His, Thr66His, Leu25Met, Asp9Leu
Trx[Bc]-3.1.1	Trx[Bc]-3.1 + His12Phe
Trx[Bc]-3.1.2	Trx[Bc]-3.1 + His66Ile
Trx[Bc]-3.1.3	Trx[Bc]-3.1 + Met25Val
Trx[Bc]-4.0.1	Trx[Bc]-3.1 + Tyr70Phe
Trx[Bc]-4.0.2	Trx[Bc]-3.1 + Asn63Ala
Trx[Bc]-4.0.3	Trx[Bc]-3.1 + Lys69Ala
Trx[Bc]-4.1 ^e	Trx[Bc]-3.1 + Leu7His + His12Ala
Trx[Bc]-4.1.1	Trx[Bc]-4.1 + Met25Val
Trx[Bc]-4.2.1	Trx[Bc]-3.1 + Tyr70Trp
Trx[Bc]-4.2.2	Trx[Bc]-3.1 + Leu17Trp
Trx[Bc]-4.2.3	Trx[Bc]-3.1 + Lys69Trp
Trx[Bc]-4.2.4	Trx[Bc]-3.1 + Leu17Trp, Lys69Trp
Trx[Bc]-4.2.5	Trx[Bc]-4.1 + Val16Met
Trx[Bc]-4.2.6	Trx[Bc]-4.1 + Phe27Met
Trx[Bc]-4.2.7	Trx[Bc]-4.1 + Val16Met, Phe27Met
Trx[Bc]-4.3.1	Trx[Bc]-3.1 + Val16Ile, Phe27Val
Trx[Bc]-4.3.2	Trx[Bc]-3.1 + Val16Ile, Phe27Ile
Trx[Bc]-4.3.3	Trx[Bc]-3.1 + Val16Leu, Phe27Ile
Trx[Bc]-4.3.4	Trx[Bc]-3.1 + Val16Phe, Phe27Ile
Trx[Bc]-4.3.5	Trx[Bc]-3.1 + Val16Phe
Trx[Bc]-4.3.6	Trx[Bc]-3.1 + Val16Ile
Trx[Bc]-4.3.7	Trx[Bc]-3.1 + Val16Leu
Trx[Bc]-4.3.8	Trx[Bc]-3.1 + Phe27Ile
Trx[Bc]-4.3.9	Trx[Bc]-3.1 + Phe27Ile
Trx[Bc]-4.4 ^e	Trx[Bc]-3.1 + Leu7Met + Met25Val
Trx[Bc]-4.5.1	Trx[Bc]-3.1 + Met25His
Trx[Bc]-4.5.2	Trx[Bc]-3.1 + Met25Asp
Trx[Bc]-4.5.3	Trx[Bc]-3.1 + Met25Asn
Trx[Bc]-4.5.4	Trx[Bc]-3.1 + Met25Glu
Trx[Bc]-4.5.5	Trx[Bc]-3.1 + Met25Gln

^a The first number in the name of the mutants refers to the design cycle in which it was constructed. The second number groups it by experiment, the third by version. ^b Cumulative mutations relative to a preceding construct are shown. ^c Mutations are relative to the wild-type sequence of *E. coli* thioredoxin. ^d First described by Hellinga et al.¹¹ ^e Primary design (unique primary coordination sphere).

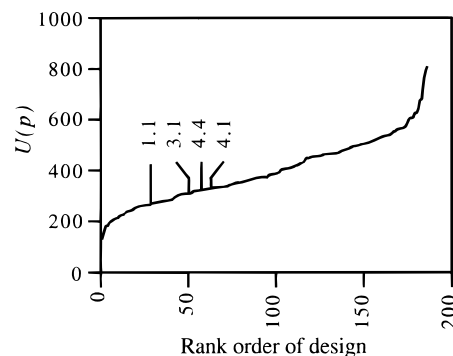


Figure 2. Rank ordering of the designs (*x*-axis) according to the weighted least-squares deviation from ideal tetrahedral geometry of the model [$U(p)$ score]. The $U(p)$ scores of the four primary designs that were tested experimentally are indicated on the curve (numbers indicate the construct; see Table 1).

and argon-purged solutions. To obtain molar extinction coefficients, the absorbances of the complexes were normalized to the concentration of free thiols measured prior to metal addition. To obtain maximum absorbances, and to estimate binding constants, the absorbances were fit to a binding isotherm, as described previously.⁸

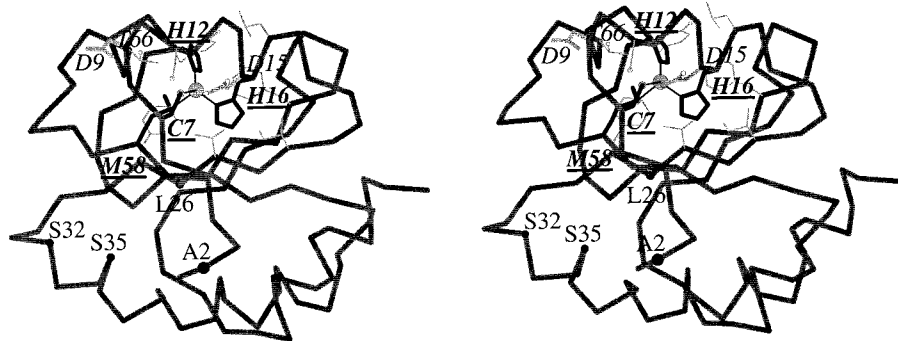


Figure 3. Stereoview of the Trx[Bc]-1.1 design. The residues Cys(C)7, His(H)12, His(H)16, and Met(M)58 (all underlined) are designed to form the primary coordination sphere. The residues in the immediate vicinity of the designed coordination sphere are indicated in thin gray lines to convey an impression of the local packing interactions. The Cys32Ser(S), Cys35Ser(S) double mutant removes the native disulfide bridge, leaving Cys7 as the only thiol in the protein. Mutation Asp2Ala(A) removes an adventitious surface copper-binding site. Asp26Leu(L) is a mutation known to increase the general stability of the protein. Residues Asp(D)9 and Asp(D)15 (*italics*) form a competing coordination sphere that is removed successfully by mutagenesis in design Trx[Bc]-2.4. Thr66(T) is changed to Ile in Trx[Bc]-2.4.

Results

Design of Blue Copper Sites in the Hydrophobic Core of Thioredoxin. The automated rational protein design program, Dezymer,⁴ was used to predict locations of mutations to introduce distorted tetrahedral CysHis₂Met sites in *E. coli* thioredoxin based on its high-resolution X-ray structure.⁵ Dezymer systematically examines a three-dimensional structure to identify sites where appropriate amino acids can be placed to introduce a coordination sphere of predetermined geometry while maintaining steric compatibility with the protein fold. The protein backbone is kept fixed throughout the search. The algorithm uses a simple description of molecular interactions in which the primary coordination sphere of the metal is described in purely geometrical terms (bond lengths, angles, torsional relationships) and all other, nonbonded interactions by a hard-sphere model. At the conclusion of the search, the sites are rank-ordered according to a score, $U(p)$, that reflects the least-squares deviation of the modeled center from the ideal geometry.³⁴

There are $108 \times 107 \times 106 \times 105 = 1.3 \times 10^8$ possible ways to place four residues in the 108-residue chain of thioredoxin, and $\sim 10^{13}$ ways of doing so if the minimum number of possible amino acid side-chain rotamers needed to represent the structure of these residues are also taken into account. About 200 candidates that form a geometrically reasonable CysHis₂Met coordination sphere were identified by the Dezymer program, representing a 10^{11} -fold enrichment over the theoretical total number of candidates. The sites used in this study were selected from the subset of sites that have reasonable geometries as reflected by a low $U(p)$ score (Figure 2), as well as other design criteria as described below for each design cycle.

Design Cycle 1. The first site to be constructed in thioredoxin, Trx[Bc]-1.1 (Table 1), was chosen because this site has a low $U(p)$ score, it is buried in the hydrophobic core (Figure 3), and the four mutations required to construct the primary coordination sphere (Leu7Cys, Val12His, Phe16His, and Leu58Met) are predicted to be sterically compatible with the surrounding residues so that no additional mutations are required. This design tests whether a primary coordination can be introduced into thioredoxin and whether this is sufficient to reproduce the dominant features of the desired metal coordination, thereby providing an entry point into the iterative design

(34) $U(p) = 0$ means the predicted geometry in a design is identical to the geometry around the Cu(II) center in plastocyanin. $U(p) > 0$ is nonideal; an arbitrary cutoff of $U(p) > 500$ is deemed unacceptable in the weighting scheme used in this particular search.

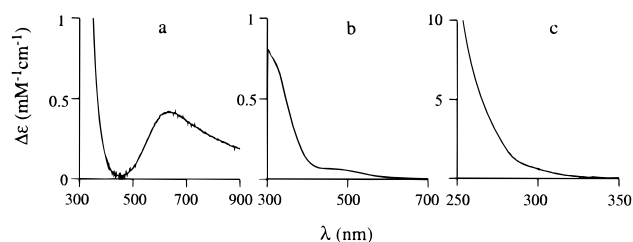


Figure 4. Electronic absorption spectra^{35,36} of Cu(II) (a), Co(II) (b), and Hg(II) (c) complexes of the Trx[bc]-1.1 design.

procedure. The properties of this site have been described previously.¹¹ Here the main findings are outlined and additional data on the Co(II) complex are presented.

The M13 construct of Trx[Bc]-1.1 was able to grow on the $\Delta trxA$ strain A307, indicating that the mutant was able to adopt a native, thioredoxin-like protein fold. Metal complexes were prepared by direct addition to purified fusion protein. The electronic absorption spectra of the Cu(II) and Hg(II) complexes have been described in detail previously.^{11,35} Briefly, the Cu(II) complex (Figure 4a) does not show the strong absorbances normally associated with LMCT bands that are indicative of the formation of Cu(II)/thiolate coordination in type 1, type 2, or type 1.5 centers.^{17,25} Instead the absorbances are broad, relatively weak absorbances in the 550–900-nm range, and strong in the 300–350-nm region, which are characteristic of $d-d$ transitions and LMCT interactions between Cu(II) and imidazole (histidine) respectively.³⁷ The spectrum of the Hg(II) complex (Figure 4b) is similar to a plastocyanin–Hg(II) complex³⁸ and consistent with thiolate coordination in a four-coordinate environment.³⁹ The Co(II) spectrum (Figure 4c) shows a strong absorbance at ~ 320 nm, indicating thiolate coordination,⁴⁰ but the intensities and energies of the $d-d$ transitions in the 400–500-nm region are consistent with the formation of a five- or six-coordinate complex, rather than the

(35) The spectra of the metal complexes presented here were obtained by using the Maltase Binding Protein fusion protein. Previously published spectra were obtained by using the mutant thioredoxin domain itself.

(36) $\Delta\epsilon$ is the normalized difference absorbance obtained after subtracting the absorbance contribution by the apoprotein.

(37) Fawcett, T. G.; Bernarducci, E. E.; Krogh-Jespersen, K.; Schugar, H. J. *J. Am. Chem. Soc.* **1980**, *102*, 2598–2604.

(38) Tamilarasan, R.; McMillin, D. R. *Inorg. Chem.* **1986**, *25*, 2037–2040.

(39) (a) Wright, J. G.; Natan, M. J.; MacDonnell, F. M.; Ralston, D. M.; O'Halloran, T. V. *Prog. Inorg. Chem.* **1990**, *38*, 323–412. (b) Utschig, L. M.; Wright, J. G.; O'Halloran, T. V. *Methods Enzymol.* **1993**, *226*, 71–97.

(40) Maret, W.; Vallee, B. L. *Methods Enzymol.* **1993**, *226*, 52–71.

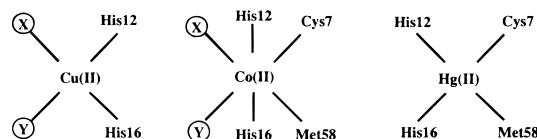


Figure 5. Interpretation of the metal complexes formed in Trx[Bc]-1.1. One or two putative alternative ligands (X,Y) can form a competing site or extend the designed coordination sphere.

intended four-coordinate tetrahedral complex.⁴¹ Furthermore, it had been shown previously that Hg(II) is a competitive inhibitor of Cu(II) binding, and that the EPR spectrum of the Cu(II) complex is consistent with N_2O_2 rather than N_2S_2 coordination.¹¹

These results can be interpreted in terms of a model in which, in addition to the designed coordination sphere, one or two other ligands can have access to the site, forming either a competing site, or expanding the coordination number (Figure 5). In this interpretation, Hg(II) is postulated to bind in the designed site as intended, consistent with its strong preference for soft ligands such as the thiol and thioether. Co(II) also binds to all four residues in the designed coordination sphere, but in addition recruits one or two other ligands, forming a five- or six-coordinate site. Cu(II) is postulated to bind to the two histidines (accounting for the competitive inhibition by Hg(II)), but ignores the two soft ligands in preference to one or two other ligands.

This model suggests that, although the designed site is able to present the intended geometry [the Hg(II) complex forms correctly], construction of a geometrically correctly formed primary coordination is not sufficient, because there is a dominant competing state in which additional ligands can extend the coordination sphere in the case of the Cu(II) and Co(II) complexes. This model can be tested experimentally and suggests a negative design strategy to constrain coordination by removing the competing ligands in the next iteration of the design cycle.

Design Cycle 2: Elimination of Competing Coordination Sphere. The ligands that form part of the unwanted, competing coordination sphere in Trx[Bc]-1.1 can potentially come from several different sources: other amino acid side chains, main-chain carbonyls or amides, and solvent components (water, counterions, buffer ions). Examination of the Trx[Bc]-1.1 model suggests that the nearby Asp9 or Asp15 could rearrange, allowing one or both carboxylates to participate in the competing coordination sphere (Figure 3). To test this hypothesis, these carboxylates were removed by mutating Asp9 and Asp15 to leucine, which is approximately isosteric to aspartate. Asp9 is rather unusual in that it is partly buried in the core of the protein, forming a hydrogen bond with Thr66. To avoid leaving a deleterious unsatisfied hydrogen bond in the hydrophobic core, an Asp9Leu Thr66Ile double mutant was also constructed. Isoleucine, rather than isosteric valine, was chosen to replace Thr66 because this slightly improved the packing around the designed site. Four different versions were constructed: three single aspartate mutants (Trx[Bc]-2.1, Trx[Bc]-2.2, Trx[Bc]-2.3), and a double aspartate mutant (Trx[Bc]-2.4) that also contains the Thr66Ile mutation. The M13 construct of Trx[Bc]-2.4 was able to support phage growth, indicating that it forms a native-like folded structure.

The spectra of the Co(II) complexes of the two single aspartate mutants (Trx[Bc]-2.1, Trx[Bc]-2.2, Trx[Bc]-2.3) are similar to the Co(II) complex of Trx[Bc]-1.1. However, the spectrum of the Co(II) complex of the Trx[Bc]-2.4 double

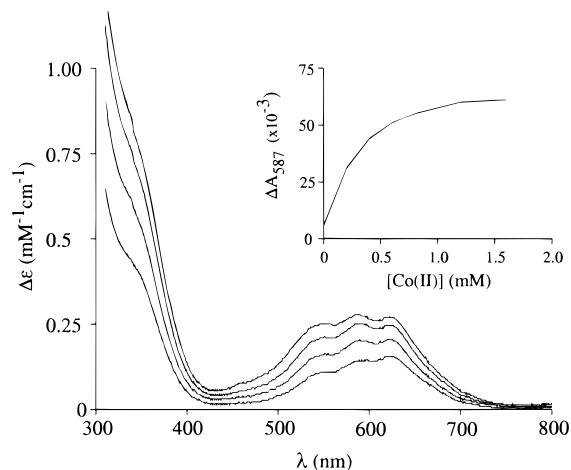


Figure 6. Electronic absorbance spectra³⁶ of the Trx[bc]-2.4-Co(II) complex formed by direct titration of the apoprotein with $CoCl_2$. Inset: change of absorbance at 587 nm (ΔA_{587}) upon addition of Co(II). $K_d(Co) = 250 \mu M$ was obtained by fitting to a binding isotherm. Titration of 1 equiv of $ZnCl_2$ or $HgCl_2$ completely eliminated absorbances in the 350- and 600-nm regions (not shown). All titrations were done with 0.23 mM protein in a solution of 50 mM Tris-chloride (pH 7.5), 200 mM NaCl.

aspartate mutant shows absorption bands in the 500–700-nm region of energies, intensities and line-shape characteristic of $d-d$ transitions expected for a tetrahedral coordination geometry,⁴¹ and a strong absorbance in the 320-nm region, indicative of a LMCT due to thiol coordination⁴⁰ (Figure 6). These results, therefore, are consistent with the hypothesis that the coordination geometry in the Trx[Bc]-1.1 construct is dominated by the presence of an alternative, competing coordination sphere that includes both Asp9 and Asp10 carboxylates. Once these potential ligands have been removed, a site with the intended Co(II) coordination number and geometry is formed.

However, unlike Trx[Bc]-1.1, Trx[Bc]-2.4 does not form a stable Cu(II) complex. Instead, SDS/PAGE reveals that addition of Cu(II) (either aerobically or anaerobically) results in the formation of a species of approximately twice the molecular weight of the fusion protein. Addition of 10 mM dithiothreitol to this product restores the molecular weight to that of the monomeric fusion protein. This indicates that the dimer is formed by an intermolecular disulfide cross-link. Presumably this disulfide forms as a consequence of reaction 1, since, in the absence of dioxygen, Cu(II) is the only oxidizing species present. This disulfide must involve the cysteine in the designed site, as it is the only cysteine in the entire fusion protein. In the Trx[Bc]-2.4 construct, redox reaction 1 is therefore postulated to be favored in preference to the formation of a stable Cu(II)-thiolate coordination complex. Thus, even though we have now controlled the coordination number of the coordination sphere and form the intended Co(II) complex in this second design cycle, another dominant competing state has been uncovered that also needs to be eliminated.

Design Cycle 3: Elimination of Disulfide Formation. The Trx[Bc]-2.4-Co(II) complex assumes the intended geometry, indicating that the predicted structure of this protein is approximately correct and that the cysteine in the designed site is therefore located in the hydrophobic core of the protein. However, Cys7 is located near the N-terminus in the edge strand of the central β -sheet, where it could become exposed by a partial unfolding of this region, thereby making it available for the formation of the unwanted intermolecular disulfide bridge. If this model is correct, then the sum of the free energies of

(41) Bertini, I.; Luchinat, C. *Adv. Inorg. Chem.* **1984**, *6*, 71–111.

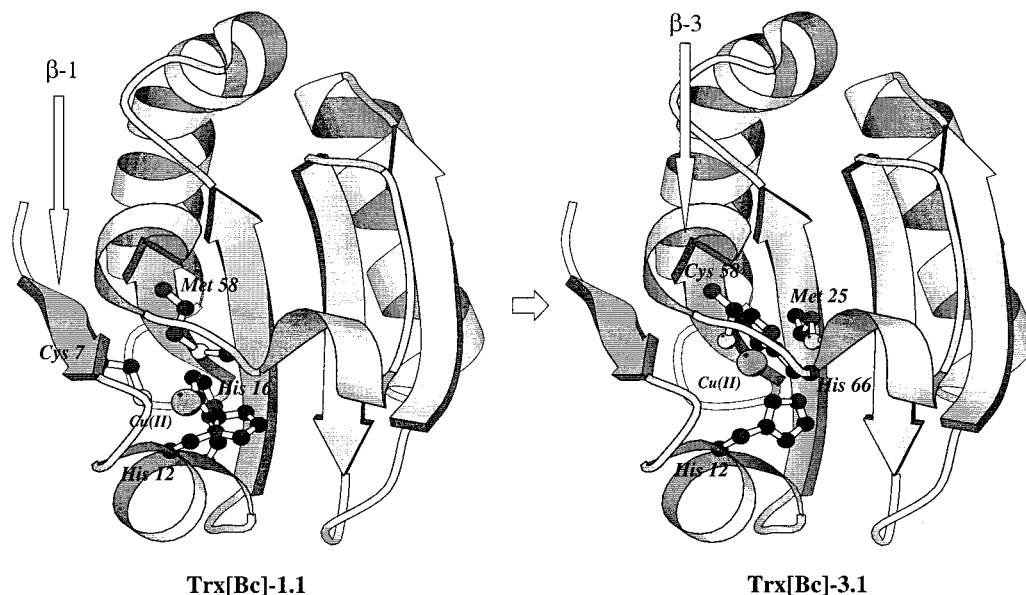


Figure 7. Comparison of the locations of the coordinating cysteine in designs Trx[Bc]-1.1 and Trx[Bc]-3.1. The location of the cysteine in the coordination sphere is moved from an edge β -strand (β -1) that can easily fray in design Trx[Bc]-1.1 to the more constrained, adjacent β -strand (β -3) in the Trx[Bc]-3.1 design.

thiol exposure (ΔG_E), the formation of the disulfide bond (ΔG_{RSSR}), and the Cu(II)/Cu(I) redox couple ($\Delta G_{Cu(II)/Cu(I)}$) exceeds the free energy of Cu(II) binding to the native state (ΔG_b).⁴²

$$\Delta G_E + \Delta G_{RSSR} + \Delta G_{Cu(II)/Cu(I)} < \Delta G_b \quad (2)$$

There are therefore two obvious strategies to reverse this inequality: lower the ΔG_b (target state optimization), or raise the ΔG_E (negative design). Of these two choices, destabilization of the free energy of the thiol exposure leads to a more straightforward design route, since ΔG_E is predicted to be equivalent to the free energy of unfolding of the region in which the cysteine is located. If the hypothesis that only a local unfolding reaction forms a barrier to thiol exposure in the Trx[Bc]-2.4 construct is correct, then placement of the cysteine in a region where a larger part of the protein has to be unfolded to expose the cysteine should result in raising ΔG_E , although it is impossible to predict the magnitude of such a change a priori.

Examination of the other solutions generated by Dezymer identified another potential buried site with reasonably low $U(p)$, Trx[Bc]-3.1. In this site the location of the Cu(II) is about the same as in Trx[Bc]-1.1, but the residues forming the primary coordination are rotated relative to the arrangement in Trx[Bc]-1.1, such that the cysteine has moved over to the next β -strand. In addition to the four residues forming the primary coordination sphere, an Asp9Leu mutation has also been introduced in Trx[Bc]-3.1 to compensate for the loss of Thr66 (with which Asp9 is hydrogen-bonded) and to eliminate a potential alternative ligand. In this construct, exposure of the thiol is now expected to require the entire domain on one side of the β -sheet to unfold (Figure 7). Trx[Bc]-3.1 is therefore predicted to favor coordination complex formation over redox chemistry by destabilization of ΔG_E relative to Trx[Bc]-2.4.

The phage growth phenotype of Trx[Bc]-3.1 indicates that it forms a native-like structure. The spectrum of the Co(II) complex (Figure 8a) is consistent with formation of the predicted tetrahedral complex and with coordination of the cysteine, based

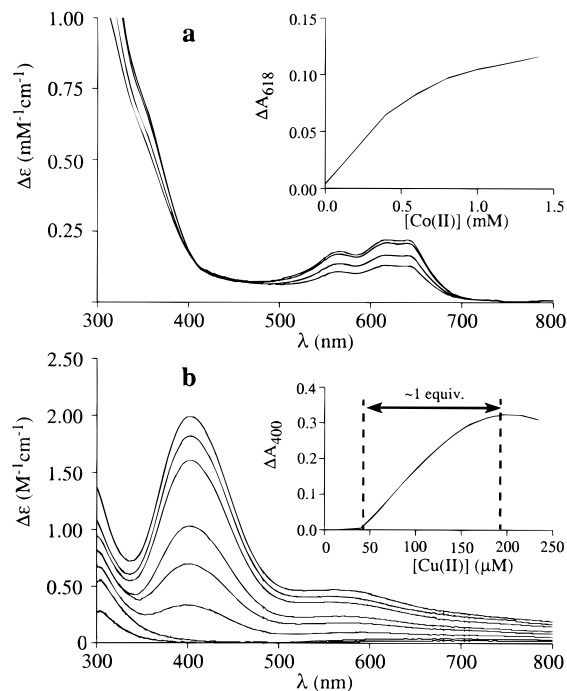


Figure 8. Electronic absorbance spectra³⁶ of the Co(II) (a) and Cu(II) (b) complexes of Trx[Bc]-3.1 formed by direct titration of the apoprotein with metal (all titrations were done in 50 mM Tris-chloride, pH 7.5, 200 mM NaCl). Inset a: change of absorbance at 618 nm upon titration with CoCl₂; protein concentration: 500 μ M; $K_d(\text{Co}) = 500 \mu\text{M}$, obtained by fitting to a binding isotherm.⁸ Inset b: change of absorbance at 400 nm upon addition of CuCl₂; protein concentration: 150 μ M; $K_d(\text{Cu}) = 1 \mu\text{M}$, obtained by fitting to a binding isotherm.⁸ Saturation of the absorbance at 400 nm is achieved by addition of 1 equiv of Cu(II) after an initial lag that is the result either of a metal-buffering effect of the Tris buffer or of a binding of Cu(II) by a second, stronger, adventitious site in the MBP-Trx[Bc]-3.1 fusion protein. Titration of 1 equiv of ZnCl₂ or HgCl₂ completely eliminates absorbances in the 350-nm and 600-nm region of the Co(II) complex and absorbance in the 400-nm region of the Cu(II) complex (not shown).

(42) Energy differences are measured relative to a solution containing apoprotein and free Cu(II).

on the absorbances in the 500–700-nm region⁴¹ and the strong absorbance in the 320-nm region⁴⁰ respectively. The Cu(II)

Table 2. Electronic Absorption Spectra of the Cu(II) and Co(II) Complexes of Selected Designs

construct	λ_{\max} nm ($\Delta\epsilon_{\lambda}$ mM ⁻¹ cm ⁻¹)	
	Cu(II) complex	Co(II) complex
Trx[Bc]-3.1	400(2.0), 560(0.46)	350(0.77 sh), 566(0.20), 620(0.24), 640(0.24)
Trx[Bc]-3.1.1	not formed	not formed
Trx[Bc]-3.1.2	not formed	not formed
Trx[Bc]-3.1.3	396(3.4), 548(0.63)	350(0.3sh), 554(0.12), 608(0.13), 635(0.12)
Trx[Bc]-3.1.3 + azide ^a	400(1.25sh), 454(2.46) 554(2.58), 795(0.48)	350(1.23sh), 548(0.26), 606(0.33), 652(0.40)
Trx[Bc]-4.0.1	392(1.49), 585 (0.37)	350(0.76sh), 566(0.19), 618(0.22), 640(0.22)
Trx[Bc]-4.0.2	400(1.4), 588 (0.31)	
Trx[Bc]-4.0.3	395(1.5), 580(0.45)	350(1.0sh), 566(0.21), 620(0.24), 640(0.22)
Trx[Bc]-4.1	397(1.49), 535(0.41)	350(0.62sh), 567(0.22), 610(0.25), 646(0.30)
Trx[Bc]-4.1.1	422(1.84), 540(0.69), 745(0.23)	350(0.55sh), 570(0.20), 610(0.23), 647(0.29)
Trx[Bc]-4.1.1 + azide ^a	438(1.51), 554(1.54), 774(0.30)	350(1.24sh), 568(0.23), 607(0.31), 654(0.40)
Trx[Bc]-4.2.1	390(2.1sh), 420(2.61), 554(0.60sh)	
Trx[Bc]-4.2.2	not formed	
Trx[Bc]-4.2.3	400(1.05), 580(0.21)	
Trx[Bc]-4.2.4	not formed	
Trx[Bc]-4.2.5	392(2.24), 543(0.61)	350(0.53sh), 570(0.21), 616(0.26), 645(0.3)
Trx[Bc]-4.2.6	392(0.48), 545(0.05)	350(0.65sh), 560(0.23), 628(0.24), 645(0.27)
Trx[Bc]-4.2.7	392(0.67), 545(0.07)	
Trx[Bc]-4.3.1	385(3.5)	
Trx[Bc]-4.3.2	382(3.1)	
Trx[Bc]-4.3.3	380(1.44)	
Trx[Bc]-4.3.8	not formed	
Trx[Bc]-4.3.9	392(2.0), 600(0.35)	350(1.4sh), 560(0.31), 594(0.36), 622(0.31)
Trx[Bc]-4.4	399(2.70), 545(0.55)	350(0.59), 560(0.15), 606(0.18), 645(0.16)
Trx[Bc]-4.5.1	not formed	not formed
Trx[Bc]-4.5.2	not formed	350(0.48sh), 540(0.17), 575(0.17), 625(0.12)
Trx[Bc]-4.5.4	not formed	350(0.76sh), 540(0.21), 590(.19), 626(0.15)
Trx[Bc]-4.5.5	not formed	350(0.8sh), 540(0.26), 590(0.23), 620(0.15)

^a Spectra of complexes formed by addition of exogenous azide to preformed Cu(II) or Co(II) metalloproteins.

complex exhibits an intense yellow color, associated with a strong absorbance band at 400 nm ($\epsilon_{400} = 2 \text{ mM}^{-1}\text{cm}^{-1}$), indicative of a LMCT attributable to the formation of a stable Cu(II)–thiolate bond¹⁶ (Figure 8b). Thus the competing redox reaction has been successfully destabilized by burying the thiol in the interior of the protein, as predicted. However, the LMCT at 400 nm indicates that the Cu(II) has adopted the more stable tetragonal, type 2 geometry, rather than type 1.^{17,25} Therefore, yet another competing state has been uncovered.

Design Cycle 4.0: Characterization of Coordination Sphere. There are two possible reasons for the formation of the unwanted geometry by the Cu(II) complex: Either all designed four residues form part of the coordination sphere, but their geometric arrangement is insufficiently constrained by packing interactions with the surrounding protein environment so that the metal forces the collapse from a tetrahedral to the more stable tetragonal arrangement; or not all residues are involved in the primary coordination sphere, and Cu(II) recruits a competing ligand. To distinguish between these two possibilities, the residues in the designed site were mutated back to their original, noncoordinating amino acids. Removal of either histidine (Trx[Bc]-3.1.1 and Trx[Bc]-3.1.2) completely destroys the binding site, and neither Co(II) nor Cu(II) binds. However, Met25Val does not affect the spectrum of the Cu(II) complex, whereas it severely distorts the Co(II) complex (Table 2). This suggests that although Met25 can participate in a tetrahedral coordination sphere, it is ignored by Cu(II) in favor of another, competing ligand (Figure 9). This competing ligand must lie in the trigonal plane formed by Cys58, His12, and His66 and be near one of the edges, thereby extending the plane to form a tetragonal complex.

The Trx[Bc]-3.1 model (Figure 10) suggests that there are no nearby main-chain carbonyl or amide bonds that could participate in formation of a tetragonal complex without severe

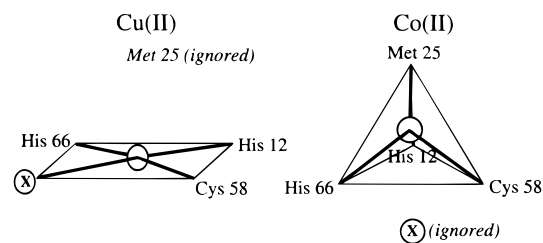


Figure 9. Postulated coordination of the Cu(II) and Co(II) complexes in the Trx[Bc]-3.1 design.

distortion of the structure. Such distortions would be expected to destabilize the protein, which is inconsistent with the observation that the cysteine is sufficiently well buried that it does not participate in the competing redox reaction. Main-chain groups were therefore ruled out as the source of the competing ligand. Three side chains located in the vicinity of the site were identified as potential alternative ligands. Each of these was mutated to remove the functional groups that could interact with the Cu(II). None of these mutations (Trx[Bc]-4.0.1 through 4.0.3) resulted in significant changes in the electronic absorption spectra of the Cu(II) or Co(II) complexes (Table 2). Participation of side chains was therefore also ruled out, leaving solvent components as the only likely source for the competing ligand. Buffer and salt conditions were changed to establish whether a buffer or a counterion participated in formation of the Cu(II) coordination sphere. All combinations of buffers (Tris, phosphate, Hepes) and counterions (chloride, sulfate, acetate, fluoride) tried gave the same Cu(II) and Co(II) electronic absorption spectra. This process of elimination leaves water (or hydroxyl) as the most likely candidate for the ligand that successfully competes with the methionine thioether to form the alternative, unintended coordination geometry.

Examination of the Trx[Bc]-3.1 model (Figure 10) shows that the Cys58/His12 and Cys58/His66 edges are bordered by well-

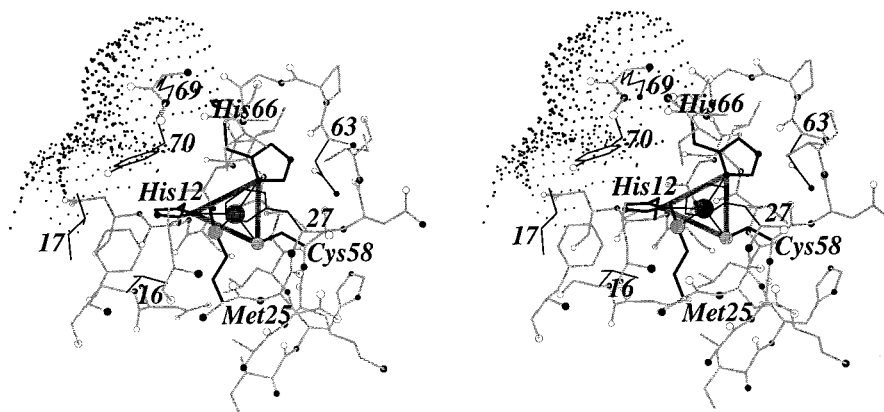


Figure 10. Stereoview of the environment of the Trx[Bc]-3.1 design. All residues located within ~ 10 Å of the Cu(II) center (large black circle) are shown. Residues Cys58, His12, and His66 form a trigonal plane (shown in thick gray lines; thin black lines show bonds to the copper), with Met25 as the weak axial ligand. Residues Asn63, Lys69, and Tyr70 were mutated to test whether they could act as competing ligands (Trx[Bc]-4.0.1 through 4.0.3). To form the observed tetragonal Cu(II) complex, the trigonal plane has to be extended by an additional vertex placed adjacent to one of the three planar edges. Two of the three edges are located in well-packed regions of the protein, but the His12–His66 edge is protected only by the surface residues Lys69 and Tyr70, which could potentially move to allow access of a water molecule. The region of the protein shown here protrudes into the solvent. The molecular view is oriented such that the observer looks out from the center of the protein. The unconnected dots outline a portion of the static solvent-accessible surface area in a region of the surface where a putative solvent channel points at the His12–His66 edge of the trigonal plane. This channel is lined by residues 17, 69, and 70 (thin black lines), which were mutated in an attempt to block the channel. A small combinatorial library was constructed of residues 16 and 27 (thin black lines) to change the packing environment around the axial methionine.

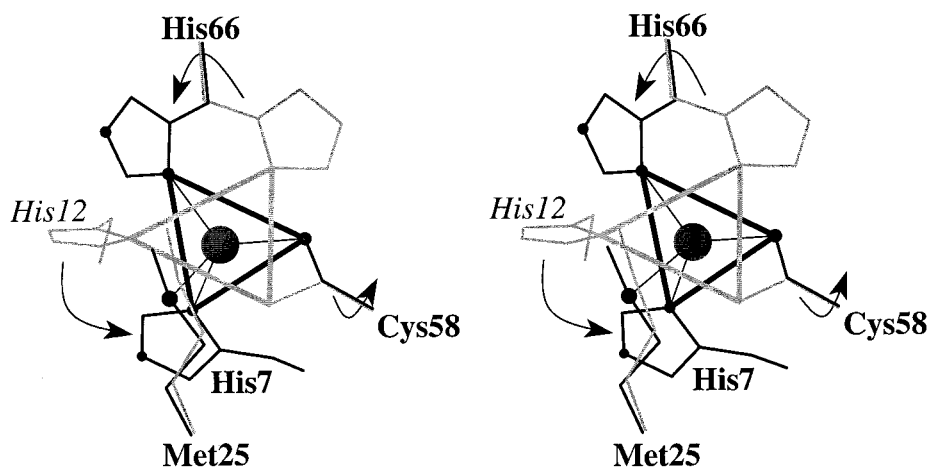


Figure 11. Stereoview showing the changes that lead to the Trx[Bc]-4.1 design (in black) from Trx[Bc]-3.1 (in gray). The CysHis₂ trigonal plane rotates $\sim 60^\circ$ relative to its position in Trx[Bc]-3.1 by moving one of the histidines from position 12 in Trx[Bc]-3.1 to position 7 in Trx[Bc]-4.1. Note that Cys58 and His66 switch to different rotameric conformations. The orientation of the molecule is identical to the presentation in Figure 10.

packed hydrophobic residues. It is therefore unlikely that an additional equatorial vertex can be sterically accommodated next to one of these edges. However, the His12/His66 edge is protected only by Lys69 and Tyr70 side chains, which are located on the surface of the protein and therefore are likely to be somewhat mobile, so that potentially they can move slightly to open up a cavity for water binding. Furthermore, such a movement could allow facile access by solvent, since it would extend a nearby solvent channel toward this vulnerable edge. Two possible strategies, therefore can be pursued in the next design cycle to form the tetrahedral Cu(II) coordination geometry: destabilization of tetragonally bound water (negative design), or stabilization of the weak axial ligand (target state optimization).

Design Cycle 4.1: Rotation and Tilting of the CysHis₂ Trigonal Plane. If the main determining factor for water binding is the local environment of the vulnerable trigonal edges, then a design in which the trigonal plane has been reoriented might eliminate water binding. There is another predicted site

with a reasonable low $U(p)$ score that is closely related to Trx[Bc]-3.1. Design Trx[Bc]-4.1 retains Cys58, His66, and Met25 (all of which adopt significantly different rotamers), but moves the second coordinating histidine from position 12 to 7. Position 12 is mutated to an alanine to avoid an unfavorable steric interaction with His66. These mutations result in a rotation of $\sim 60^\circ$ and a tilt of $\sim 15^\circ$ of the trigonal plane relative to the Trx[Bc]-3.1 design, thereby relocating the three edges of the trigonal plane in somewhat different environments (Figure 11).

Trx[Bc]-4.1 has very similar characteristics to Trx[Bc]-3.1 (Table 2). It forms a stable Cu(II)–thiolate coordination complex that still adopts the tetragonal rather than the intended distorted tetrahedral geometry, even though the Co(II) complex again shows tetrahedral geometry. Furthermore, just as for Trx[Bc]-3.1.1, loss of the axial methionine in Met25Val mutation (Trx[Bc]-4.1.1) affects the spectrum of the Co(II) but not the Cu(II) complex, indicating that Met25 can coordinate to the metal center but is ignored in the Cu(II) complex. Thus tetragonal water can be accommodated even if the trigonal plane

has been reoriented by a 60° rotation regardless of the proximity of a potentially vulnerable edge of the trigonal coordination plane to the solvent-accessible surface.

Design Cycle 4.2: Attempted Elimination of Water. Elimination of the attacking water requires that sufficiently strong local packing interactions are maintained around the designed site to sterically occlude the water from the vicinity of each of the three edges in the trigonal CysHis₂ plane. One approach is to attempt to sterically block the solvent channel located adjacent to the most vulnerable His12/His66 edge in the Trx[Bc]-3.1 design. This is not simple to achieve, because the local geometry of the chain in this region does not readily lend itself to the positioning of a bulky side-chain in the channel. Residues Leu17, Lys69, and Tyr70 line the channel (Figure 10), and were mutated singly to tryptophan in an attempt to block the channel (Trx[Bc]-4.2.1–4.2.3). A double mutant (Trx[Bc]-4.2.4) was also constructed. However, none of these constructs resulted in the elimination of the equatorial ligand (Table 2).

A similar strategy was explored with the Trx[Bc]-4.1 design as the starting point, but rather than using bulky, relatively rigid residues such as tryptophan, highly flexible methionines were tried. Val16 and Phe27 were each changed to methionine. Neither the two single mutants (Trx[Bc]-4.2.5, Trx[Bc]-4.2.6) nor the double mutant (Trx[Bc]-4.2.7) showed elimination of the bound water, although all still retained the ability to bind tetragonal Cu(II) and tetrahedral Co(II), indicating that the protein fold had not been destroyed by these mutations (Table 2). Thus the negative design approach to eliminate competing states has so far not been successful.

Design Cycle 4.3: Attempted Strengthening of the Axial Methionine. If the competing equatorial ligand cannot be eliminated by negative design, the other approach is to try and lower the free energy of the target state by strengthening the interaction with the axial ligand. The Co(II) complexes of Trx[Bc]-3.1 and Trx[Bc]-4.1 are tetrahedral and require the axial methionine to form properly. I decided to investigate whether the packing interactions around the methionine could be improved to strengthen this interaction. Met25 is wedged by two residues on either side, Val16 and Phe27, which determine its precise geometry through packing interactions, not unlike the two residues that hold the axial methionine in place in the cupredoxins.¹⁵ A small combinatorial library was constructed in which Val16 and Phe27 were replaced with several different hydrophobic residues (Trx[Bc]-4.3.1 through-4.3.9). The Co(II) electronic absorption spectra clearly indicate that these two residues influence the precise geometry of this methionine, because the relative intensities and precise energies of the three absorption bands in the *d-d* region show subtle differences while retaining their tetrahedral character^{40,41} (Table 2). However, none of these constructs resulted in the formation of a tetrahedral Cu(II) complex.

Design Cycle 4.4: Repositioning the Axial Methionine. The packing environment of the axial methionine can also be varied by repositioning it within the protein. Trx[Bc]-4.4 is derived from Trx[Bc]-3.1 by moving Met25 to position 7 on the opposite face of the trigonal plane (Figure 12). The Cu(II) and Co(II) complexes are similar to Trx[Bc]-3.1 (Table 2), indicating that even though there is yet another way of successfully presenting a tetrahedral site, the problem of eliminating the competing water has not been solved by repositioning the axial ligand.

Design Cycle 4.5: Mutants of the Axial Methionine. The thioether of the axial methionine is a weak interaction at best. None of the Blue Copper analogues obtained by building

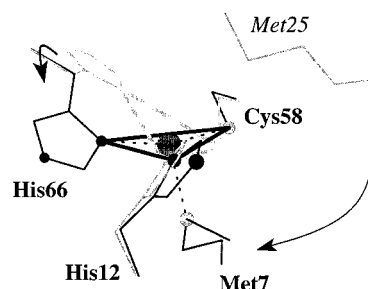


Figure 12. Sketch indicating the changes that lead to the Trx[Bc]-4.4 design (in black) from Trx[Bc]-3.1 (in gray). The axial methionine has been relocated at the opposite side of the CysHis₂ trigonal plane (Met7). Cys58 and His12 retain the same side-chain rotameric configuration as in Trx[Bc]-3.1, but His66 switches to a different rotamer. Consequently the trigonal plane (thick black lines) has been tilted relative to the original orientation of the Trx[Bc]-3.1 position. Note that Met7 occupies the location in which one of the histidines was placed in design Trx[Bc]-4.1.

synthetic models⁴³ or by protein engineering^{25,44,45} have successfully utilized such a weak interaction. Instead, strong axial ligands such as pyrazolates,⁴³ imidazoles,⁴⁴ a carboxylate,²⁵ or additional thiols²⁵ were used in these analogues. Studies with mutants of natural Blue Copper proteins have demonstrated that the axial methionine can be replaced with stronger amino acid ligands.²¹ Furthermore, one of the natural Blue Copper proteins, stellacyanin, has a glutamine in place of the usual methionine.⁴⁶

A small combinatorial library was constructed in Trx[Bc]-3.1 in which Met25 was replaced with His, Asp, Asn, Glu, or Gln (Trx[Bc]-4.5.1 through-4.5.5). Steric considerations predict that His25 does not fit well, and that Asp25 or Asn25 are too short to form a proper tetrahedral site, but that Glu25 or Gln25 should work. Trx[Bc]-4.5.1 (His25) does not bind metals as judged by direct titration, presumably because the protein has become too unstable. The electronic absorption spectrum of the Co(II) complex of Trx[Bc]-4.5.2 (Asp25) is similar to Trx[Bc]-3.1.3 (Val25), indicating that this residue does not coordinate, as expected (Table 2). The spectra of the Trx[Bc]-4.5.4 (Glu25) and Trx[Bc]-4.5.5 (Gln25) Co(II) complexes are similar to Trx[Bc]-3.1 (Met25), indicating that these two residues can form the predicted tetrahedral site (Table 2). However, none of the Trx[Bc]-4.5 series bind Cu(II). Instead, SDS/PAGE revealed that a disulfide-linked dimer forms upon addition of Cu(II). Presumably in these constructs, burial of a hydrophilic axial ligand in the hydrophobic core is so destabilizing that the free energy of folding is no longer sufficient to counteract the free energy of the competing redox reaction, and exposure of the thiol coupled to formation of the disulfide is favored over coordination complex formation, just as in Trx[Bc]-2.4. Therefore the strategy of introducing a strong axial ligand by mutagenesis fails.

(43) (a) Kitajima, N.; Fujisawa, K.; Moro-oka, Y. *J. Am. Chem. Soc.* **1990**, *112*, 3210–3212. (b) Kitajima, N.; Fujisawa, K.; Tanaka, M.; Moro-oka, Y. *J. Am. Chem. Soc.* **1992**, *114*, 9232–9233.

(44) (a) Brader, M. L.; Dunn, M. F. *J. Am. Chem. Soc.* **1990**, *112*, 4585–4587. (b) Brader, M. L.; Borchardt, D.; Dunn, M. F. *J. Am. Chem. Soc.* **1992**, *114*, 4480–4486.

(45) (a) Maret, W.; Dietrich, H.; Ruf, H.-H.; Zeppezauer, M. *J. Inorg. Biochem.* **1980**, *12*, 241–253. (b) Maret, W.; Zeppezauer, M.; Desideri, A.; Morpurgo, L.; Rotilio, G. *FEBS Lett.* **1981**, *136*, 72–74. (c) Maret, W.; Shiemke, A. K.; Wheeler, W. D.; Loehr, T. M.; Sanders-Loehr, J. *J. Am. Chem. Soc.* **1986**, *108*, 6351–6359. (d) Schneider, G.; Eklund, H.; Cedergren-Zeppezauer, E.; Zeppezauer, M. *Proc. Natl. Acad. Sci. U.S.A.* **1983**, *80*, 5289–5293. (e) Schneider, G.; Cedergren-Zeppezauer, E.; Knight, S.; Eklund, H.; Zeppezauer, M. *Biochemistry* **1985**, *24*, 7503–7510.

(46) Hart, P. J.; Nersissian, A. M.; Herrmann, R. G.; Nalbandyan, R. M.; Valentine, J. S.; Eisenberg, D. *Prot. Sci.* **1996**, *5*, 2175–2183.

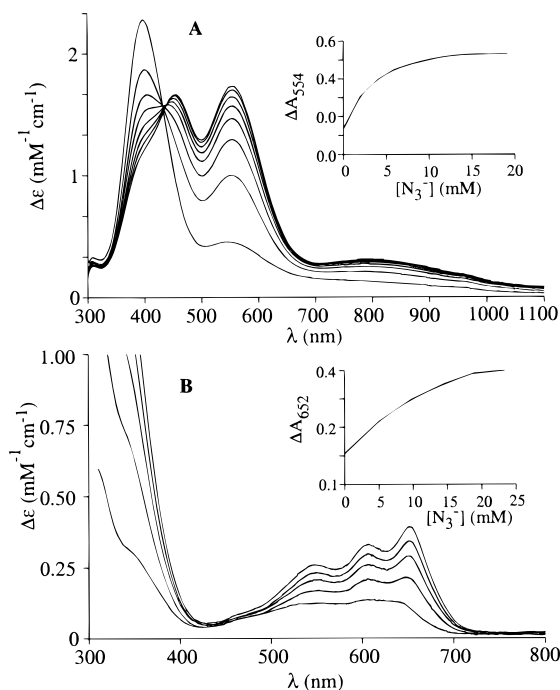


Figure 13. Electronic absorbance spectra³⁶ formed upon addition of azide to metal complexes of Trx[Bc]-3.1.1 (all titrations in 50 mM Tris-chloride, pH 7.5, 200 mM NaCl). (a) Cu(II) complex; protein concentration: 200 μ M; metal complex preformed by addition of 1 equiv of CuCl₂; inset: change of absorbance at 554 nm [$K_d(\text{N}_3^-) = 2.5$ mM]. (b) Co(II) complex; protein concentration: 510 μ M; metal complex preformed by addition of 4.4 mM CoCl₂; inset: change of absorbance at 652 nm [$K_d(\text{N}_3^-) = 7$ mM].

Design Cycle 4.6: Exogenous Axial Ligands. If the thermodynamics of protein stability prevents the introduction of a hydrophilic, strong axial ligand, the final strategy left to explore is to add an exogenous axial ligand. Such an approach has been used successfully in azurin mutants, in which the axial methionine was replaced with smaller amino acids, thereby creating a cavity in which several exogenous ligands could bind and coordinate axially.²²

Replacing Met25 with valine in the Trx[Bc]-3.1.3 and Trx[Bc]-4.1.1 variants created a small cavity above the CysHis₂ trigonal plane. The Cu(II) complexes of these variants were probed with several small ligands known to bind Cu(II), including imidazole, nitrite, nitrate, cyanide, and azide. In both variants, the yellow tetragonal Cu(II) complex changed to purple upon titration with azide (Figure 13a). Cyanide formed a purple complex only transiently, presumably because it removed the copper from the protein binding site to form a copper cyanide complex in solution. The Cu(II)/azide complexes have strong LMCT transitions at 454 and 554 nm (Table 2), similar to the spectra reported for the azide, cyanide, or thiocyanide complexes of the azurin Met121 mutants,²² which have been studied in some detail and correspond to a type 1.5 site, in which the Cu(II) is located in a tetrahedral site and is pulled above the trigonal plane by the strong axial ligand.²⁴ The electronic absorption spectra of the Co(II)/azide complexes showed that addition of azide forms tetrahedral sites (Figure 13b).

In the absence of exogenous ligands, the Trx[Bc]-3.1.3 complex adopts the same tetragonal geometry (Table 2) as its parent construct (Trx[Bc]-3.1), as expected. In contrast, the Cu(II) complex of Trx[Bc]-4.1.1 is distinct from its Trx[Bc]-4.1 parent (Figure 14). The thiol→Cu(II) LMCT at 397 nm shifts to a longer wavelength in Trx[Bc]-4.1.1 (422 nm). The 540-nm band becomes more intense relative to the 422-nm

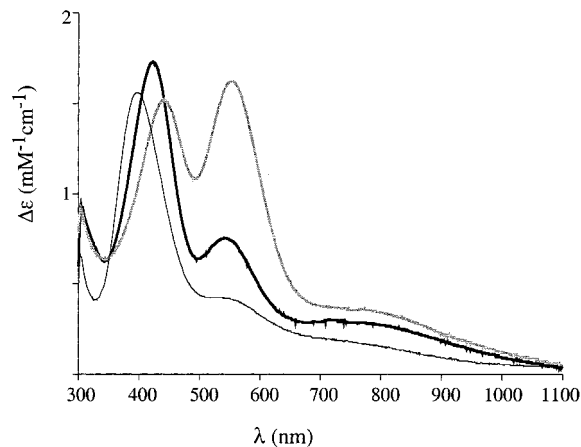


Figure 14. Comparison of the electronic absorbance spectra³⁶ of the Cu(II) complexes of Trx[Bc]-4.1 (thin line), Trx[Bc]-4.1.1 (thick line), and the Tr[Bc]-4.1.1-Cu(II)azide complex (gray line).

band: $\epsilon_{422}/\epsilon_{540} = 2.67$, compared with $\epsilon_{397}/\epsilon_{535} = 3.64$ in Trx[Bc]-4.1. In the Trx[Bc]-4.1.1 Cu(II)/azide complex, the ratio of these bands is 1.02. This ratio correlates with the type of Blue Copper site formed,^{25b} indicating that the Trx[Bc]-4.1.1 variant may have assumed some type 1.5 character, presumably as the result of water binding in the cavity created by the Met25Val mutation. Furthermore, unlike Trx[Bc]-3.1.3, the electronic absorbance spectrum of the Trx[Bc]-4.1.1-Co(II) complex shows clear tetrahedral character in the absence of azide, (Table 2).

These results suggest that strong axial ligands successfully compete with the tetragonally bound water to form the desired tetrahedral sites. Apparently, thermodynamic balance between the tetragonal and tetrahedral forms can be subtle. For Trx[Bc]-4.1.1, the relative binding constants for water in the axial cavity created by the Met25Val mutation and the postulated tetragonal binding site are such that the water apparently binds axially, thereby forming an approximate type 1.5 site without requiring introduction of a strong azide ligand (although the latter forms a much-better-defined tetrahedral site). The strategy of adding an exogenous strong axial ligand was successful, and type 1.5 Blue Copper sites can be engineered into the hydrophobic core of thioredoxin. A more detailed spectroscopic characterization of these complexes will be published elsewhere.

Discussion

In this study, I explored the factors required to introduce a Blue Copper center de novo into a protein framework that contains no a priori evolved features to accommodate a metal center, in contrast to other methods by which Blue Copper sites were created in other studies: by metal substitution in one of the zinc sites of alcohol dehydrogenase,⁴⁵ by exogenous thiol addition to Cu(II)-insulin,⁴⁴ by exploitation of structural homology relationships to transplant sites between related proteins,⁴⁷ or by reengineering a natural binding site in yeast superoxide dismutase²⁵ (SOD). The α/β fold of thioredoxin has no similarity to the β -barrel of the cupredoxins. The designed sites

(47) (a) van der Oost, J.; Lappalainen, P.; Musacchio, A.; Warne, A.; Lermieux, L.; Rumbley, J.; Gennis, R. B.; Aasa, R.; Pascher, T.; Malmström, B. G.; Saraste, M. *EMBO J.* **1992**, *11*, 3209–3217. (b) Dennison, C.; Vijgenboom, E.; de Vries, S.; van der Oost, J.; Canters, G. W. *FEBS Lett.* **1995**, *365*, 92–94. (c) Wilmanns, M.; Lappalainen, P.; Kelly, M.; Sauer-Eriksson, E.; Saraste, M. *Proc. Natl. Acad. Sci. U.S.A.* **1995**, *92*, 11955–11959. (d) Hay, M.; Richards, J. H.; Lu, Y. *Proc. Natl. Acad. Sci. U.S.A.* **1996**, *93*, 461–464. (e) Dennison, C.; Vijgenboom, E.; Hagen, W. R.; Canters, G. W. *J. Am. Chem. Soc.* **1996**, *118*, 7406–7407.

are therefore located in a completely different secondary structure environment compared with that of the natural proteins. Furthermore, a Blue Copper sequence pattern derived from cupredoxins,^{15,48} His X₋₇₀ Cys X His X₂₋₄ Met,⁴⁹ is completely distinct from the designs in thioredoxin both in order and spacing: His X₁₂ Met X₃₀ Cys X₆ His (Trx[Bc]-3.1), His X₁₇ Met X₃₀ Cys X₆ His (Trx[Bc]-4.1), and Met X₄ His X₃₀ Cys X₆ His (Trx[Bc]-4.4). The construction of a stable Blue Copper coordination sphere required destabilization of several competing coordination geometries or redox reactions. In the iterative design procedure described here, such competing states were uncovered experimentally and design strategies were developed to deal with them. In the following, I compare the results of these strategies with the natural Blue Copper proteins and their engineered variants, and with synthetic models.

Control of Primary Coordination Sphere Composition.

The first design (Trx[Bc]-1.0) presents an example of improper control of ligand selection owing to the presence of additional amino side chains that extend the designed coordination sphere. Replacement of the two interfering residues with leucine removes these unintended, competing interactions (Trx[Bc]-2.4), resulting in a hydrophobic shell surrounding the metal center. Such shells have been observed around many natural metal binding sites.⁵⁰ One interpretation is that these regions are rigid and preform the coordination sphere, thereby increasing the intrinsic affinity of the site for the metal. The results obtained in the designs presented here suggest that hydrophobic shells may play an additional role by controlling ligand access to the primary coordination sphere. Hydrophobic shells may therefore represent a natural negative design feature that controls coordination number in metal centers.

Control of Thiol Reactivity. Formation of a Cu(II)-thiolate bond is one of the main obstacles encountered in the construction of Blue Copper centers because it requires that the coordination complex be more stable than the normally highly favored redox reaction **1**. Many of the Blue Copper synthetic models are constructed by coordinating the Cu(II) in a three- or four-coordinate ligand followed by addition of an exogenous mercaptide.¹⁸ Destabilization of the redox reaction is achieved in these synthetic models by a combination of low temperatures and structural features in which Cu(II) is coordinated by a ligand that sterically occludes the reaction of two mercaptides at the copper center.⁵¹ A series of hindered tris(pyrazolylborate) Cu(II)-thiolate complexes has been particularly successful in mimicking the electronic properties of the Blue Copper sites.⁴³

An analogous strategy can be adopted in proteins by burying the thiol in the interior to suppress the redox reaction, as illustrated by designs Trx[Bc]-3.1, Trx[Bc]-4.1 and Trx[Bc]-4.4. Unlike their predecessors, these designs form a stable thiolate-Cu(II) bond. Presumably, proper placement of the cysteine requires the entire protein to unfold to expose the thiol, the free energy of such an unfolding transition being sufficient to oppose the redox reaction (eq 2). This hypothesis is further supported by designs Trx[Bc]-4.5.1 through 4.5.4, which are derivatives of Trx[Bc]-3.1 in which the buried Met25 is replaced by hydrophilic residues. None of these proteins form stable thiolate-Cu(II) coordination complexes, presumably because the stability of the protein has been decreased by the introduction

of a buried hydrophilic group to such an extent that the free energy of folding no longer exceeds that of the redox reaction (a quantitative analysis of the stabilities of these proteins will be published elsewhere).

These designs therefore suggest that it is important to bury the cysteine in such a way that it "recruits" the free energy of folding of the entire protein to oppose the redox reaction. This constraint is also clearly observable in the structure of natural Blue Copper proteins. In the general cupredoxin fold¹⁵ the cysteine in the binding site is located on a β -strand that forms part of a β -barrel that has no edge strand. Exposure of the thiol would therefore involve substantial unfolding of the protein. In addition to the hydrogen bonds formed with the main-chains of its β -strand neighbors, this strand is also stabilized by hydrogen bonds between the side chains of a pair of largely conserved residues located on the cysteine strand and an adjacent strand.⁵² The stability of this region is further emphasized by the observation that the axial methionine in azurin can be replaced with hydrophilic and charged residues without destroying the ability of this protein to form a Cu(II)-thiolate coordination complex.²¹ The Blue Copper sites that have been constructed by metal substitution in alcohol dehydrogenase,⁴⁵ exogenous thiol addition to Cu(II)-insulin,⁴⁴ or redesign of a natural metal binding site in yeast SOD²⁵ are all located in buried, rigid regions of their host protein.

Solvent Exclusion. The importance of solvent exclusion for the control of the coordination number and geometry of the Blue Copper center is clearly illustrated by the synthetic models. The tris(pyrazolylborate) Cu(II)-thiolate complexes are stable only in noncoordinating solvents such as toluene or pentane, whereas addition of even small amounts of a coordinating solvent such as dimethyl sulfoxide or dimethylformamide alters metal coordination.⁴³ A related problem is encountered in designs Trx[Bc]-3.1, Trx[Bc]-4.1, and Trx[Bc]-4.4, where the stable Cu(II)-thiolate complexes are tetragonal because the weak axial methionine ligand is discarded in preference to a strong equatorial solvent molecule. Elimination of the attacking water requires that it be sterically occluded from positions next to the edges of the CysHis₂ trigonal plane. Presumably this can be achieved by constructing strong local-packing interactions in that region. Despite several attempts, however, this negative design strategy has not yet been successful in the designs presented here. Instead, a target state optimization strategy introduced a strong (exogenous) ligand that successfully competed with the equatorial water (design cycle 4.6).

The sites engineered in insulin⁴⁴ and yeast SOD²⁵ apparently prevent solvent coordination by a combination of coordination-sphere stabilization (target state optimization) using strong ligands (N₃S in the case of insulin, and ON₂S in the case of SOD) and steric exclusion (negative design), burying the site deeply within well-packed regions of the host protein. In insulin the site lies within the trimer interface and is completely protected from solvent once the thiophenol is bound. In SOD, the Blue Copper site is the reengineered zinc site, buried in the interior of the protein.

The strategy of using strong ligands to form the coordination sphere does not recapitulate the natural mechanism of solvent exclusion, since most natural Blue Copper proteins use a weak axial thioether ligand. Nor is steric exclusion of solvent achieved in naturally evolved Blue Copper centers by the simple expedient of burying the site deeply in the interior of the protein, since they are located just beneath the solvent-accessible surface

(48) Ouzounis, C.; Sander, C. *FEBS Lett.* **1991**, *279*, 73-78.

(49) X_n indicates the spacing; the underlined section corresponds to the loop in cupredoxin that contains the Blue Copper sites.

(50) Yamashita, M. M.; Wesson, L.; Eisenman, G.; Eisenberg, D. *Proc. Natl. Acad. Sci. U.S.A.* **1990**, *87*, 5648-5652.

(51) Hughey, J. L. IV; Fawcett, T. G.; Rudich, S. M.; Lalancette, R. A.; Potenza, J. A.; Schugar, H. J. *J. Am. Chem. Soc.* **1979**, *101*, 2617-2623.

(52) Hoitink, C. W.; Canters, G. W. *J. Biol. Chem.* **1992**, *267*, 13836-13842.

of the protein. The X-ray structure of azurin⁵³ reveals that one of the edges of the trigonal plane in azurin (between His46 and His117) is particularly vulnerable to an equatorial attack by water, being shielded from solvent only by the side chains of Met44 and Met13, which form a hydrophobic patch to which redox partners can bind.⁵⁴ Furthermore, one of the histidines in the primary coordination sphere, His117, directly excludes solvent. A His117Gly mutant²⁰ opens a solvent-accessible channel, thereby forming a type 2 tetragonal complex (analogous to designs Trx[Bc]-3.1 and its derivatives). This suggests that two solvent molecules must have entered the site, one replacing His117, the other completing the tetragonal complex, presumably because the glycine has increased the flexibility of the site^{20e} and thereby allowed room for additional water. The original coordination geometry can be restored by adding exogenous ligands that mimic His117 coordination and close the channel.^{20b} Mutation of the second histidine (deeply buried in the interior of the protein) to glycine (His46Gly) also destabilizes the site such that water is internalized, resulting in type 2 Cu(II) coordination²³, thereby demonstrating that incorporation of water in the primary coordination sphere does not require a channel to the bulk solvent. The delicate balance between the Blue Copper coordination sphere and the tetragonal form is therefore easily perturbed if water is not rigorously excluded.

One of the striking structural features of Blue Copper proteins is that the binding site is remarkably rigid, as shown by the observation that the apoprotein⁵⁵ and metal-substituted⁵⁶ protein structures are very similar to that of the copper complex. This was originally taken as one of the lines of evidence that the geometry of the Cu(II) is strained and that this strain is imposed by the rigidity of the binding site.⁵⁷ This view has recently been challenged by electronic structure calculations that suggest that the Cu(II) geometry is not strained in Blue Copper sites.⁵⁸ Rather than imposing a strained geometry on the copper (a target state optimization feature), the rigidity of the site therefore may reflect a structural negative design feature that destabilizes the tetragonal form and prevents water from binding by locating the Cu(II) in a strictly "anhydrous chamber". The rigidity of this site is the consequence of several factors, including packing interactions and a network of hydrogen bonds that stabilize the residues in the primary coordination sphere and the surrounding region.^{53,59}

Conclusions

The formation of Blue Copper sites is controlled by a combination of factors that stabilize the primary coordination

sphere (target state optimization) and destabilize potential competing reactions (negative design). Negative design features are particularly important in these sites, by raising the free energy of states that are normally more stable than the unusual coordination complex achieved in the Blue Copper environment. The iterative design cycles presented here have experimentally identified three dominant factors that need to be controlled and suggest a clear path for future designs, which involves the construction of long-range interactions beyond a geometrically correct, sterically compatible primary coordination sphere. First, a hydrophobic shell surrounding the metal center prevents potential coordination of alternative ligands. Second, formation of a stable Cu(II)–thiolate bond requires destabilization of a competing thiol oxidation reaction. This can be achieved by burial of the thiol within the hydrophobic core, presumably via a mechanism in which the free energy of protein unfolding opposes the redox reaction. Third, access of ligands (in particular solvent) that can form a stable tetragonal coordination geometry must be excluded. In natural systems this is apparently achieved by a highly rigid environment that prevents relaxation of the protein matrix and thereby blocks access of small ligands. This feature was not reproduced in the designs presented here, instead, a strong exogenous axial ligand was used to stabilize a tetrahedral geometry. The next challenge in the de novo design of a Blue Copper center in thioredoxin is to construct a rigid, anhydrous chamber. This will require the introduction of cooperatively interacting residues in a secondary shell around the primary coordination sphere.

Rational design studies have shown that negative design is an important factor in the formation of unique, folded conformations.²⁸ Similarly, in addition to providing appropriately placed functional groups that lead to substrate binding and stabilization of the transition state, enzyme active sites are now recognized to suppress unwanted alternative reactions by the exclusion of water, prevention of the formation of substrate conformations that lead to decomposition, and so on. These negative design features are therefore also a crucial, if cryptic, aspect of enzyme mechanisms.

Negative design features are particularly difficult to study in natural systems for two reasons. First, the protein has evolved features to suppress the competing states, so that identifying them by study of a highly optimized natural system will be difficult. Second, the structural features to control these states may not involve obvious local interactions that can be identified by inspection and tested by mutagenesis. The Blue Copper centers provide an excellent model system for the study of negative design, because the competing states are well defined, are readily characterized by experiment, and capture many of the general aspects of the control of functional specificity encountered in enzyme systems. Rational design approaches are likely to play an increasingly important part in elucidating the role of negative design in biological structure and function.

Acknowledgment. I thank V.J. Zhang for technical assistance in mutant construction and protein purification, and T.G. Oas, D.E. Benson, and J.S. Richardson for stimulating discussions. This work was supported by a grant from the National Institutes of Health R29GM49871.

(53) Baker, E. N. *J. Mol. Biol.* **1988**, *203*, 1071–1095.

(54) van der Kamp, M.; Floris, R.; Hali, F. C.; Canters, G. W. *J. Am. Chem. Soc.* **1990**, *112*, 907–908.

(55) (a) Garrett, T. P. J.; Clingeffer, D. J.; Guss, J. M.; Rogers, S. J.; Freeman, H. C. *J. Biol. Chem.* **1984**, *259*, 2822–2825. (b) Nar, H.; Messerschmidt, A.; Huber, R.; van der Kamp, M.; Canters, G. W. *FEBS Lett.* **1992**, *306*, 119–124.

(56) (a) Church, W. B.; Guss, J. M.; Potter, J. J.; Freeman, H. C. *J. Biol. Chem.* **1986**, *261*, 234–237. (b) Nar, H.; Huber, R.; Messerschmidt, A.; Filipou, A. C.; Barth, M.; Jaquinod, M.; Kamp, M. v. d.; Canters, G. W. *Eur. J. Biochem.* **1992**, *205*, 1123–1129. (c) Moratal, J. M.; Romero, A.; Salgado, J.; Perales-Alarcón, A.; Jiménez, H. R. *Eur. J. Biochem.* **1995**, *205*, 1123–1129. (d) Bonander, N.; Vännegård, T.; Tsai, L.-C.; Langer, V.; Nar, H.; Sjölin, L. *Prot. Struct. Funct. Genet.* **1997**, *27*, 385–394.

(57) (a) Vallee, B. L.; Williams, R. J. P. *Proc. Natl. Acad. Sci. U.S.A.* **1968**, *59*, 498–505. (b) Gray, H. B.; Malmström, B. G. *Comments Inorg. Chem.* **1983**, *2*, 203–209. (c) Malmström, B. G. *Eur. J. Biochem.* **1994**, *223*, 711–718. (d) Williams, R. J. P. *Eur. J. Biochem.* **1995**, *234*, 363–381.

(58) Ryde, U.; Olsson, M. H. M.; Pierloot, K.; Roos, B. O. *J. Mol. Biol.* **1996**, *261*, 586–596.

(59) Guss, J. M.; Freeman, H. C. *J. Mol. Biol.* **1983**, *169*, 521–563.